Analysis of Whitecap Data from TREX13

Grant B. Deane
Marine Physical Laboratory, Scripps Institution of Oceanography
UCSD
La Jolla, CA 92093-0238
phone: (858) 534-0536 fax: (858) 822-2851 email: gdeane@ucsd.edu

Award Number: N00014-14-1-0366

LONG-TERM GOALS

The long-term goal is to develop remote monitoring techniques of wave breaking that will allow prediction of the acoustical effects of bubbles beneath the sea surface as a function of acoustic frequency and wind speed. Recent work has shown that, for a given wind speed driving wave breaking, there exists a critical bubble radius that controls the frequency-dependent scattering and absorption of sound incident on the sea surface[1]. Sound at frequencies equal to or greater than the natural frequency of the bubble with a critical radius tends to be absorbed within a somewhat persistent bubble layer at the surface whereas lower frequency sound is more simply refracted by the layer. The remote monitoring of wave breaking as a function of wind speed coupled with observations of reverberation in different frequency regimes will enable models of reverberation that incorporate bubble effects to be tested, furthering the ultimate objective of predicting optimal frequency bands for acoustic instrument performance under wind-driven seas.

OBJECTIVES

The immediate objective is to develop computer-aided, image processing software to quantify the properties of whitecaps beyond the percentage of surface covered by whitecaps as a function of wind speed, traditionally denoted by the variable W. Specifically, wave breaking rate, wave breaking scale, bubble cloud injection time and whitecap decay time are all sought from automated image analysis. The dataset that has been analyzed consists of surface images taken from the R/V Sharp during the TREX13 campgain. A second objective is to combine the analyzed image data with a model for bubble persistence at the sea surface to interpret surface scattering data taken during the TREX13 experiment.

APPROACH

This section is broken down into a description of the whitecap dataset, the analysis methodology developed to generate whitecap statistics and the integration of the data into analyses of surface-scattered acoustic transmissions. Since the acoustic data belongs to other Principal Investigators, the acoustic data analysis will be done in collaboration with other PIs. As explained later, the whitecap dataset analysis is complete, but the integration of that analysis into a model for surface scattering is ongoing.

Whitecap Dataset

Video imagery of whitecaps were taken from the R/V Sharp during the daylight hours of the TREX13 campaign. An overview of the deployment configuration is shown below. The image footprint is approximately 870 m^2 with a pixel resolution of 1 – 2 cm. Position data from two GPS units was logged to provide a time series of ship orientation and the camera housing contained a navigation unit to provide magnetic heading and camera inclination.

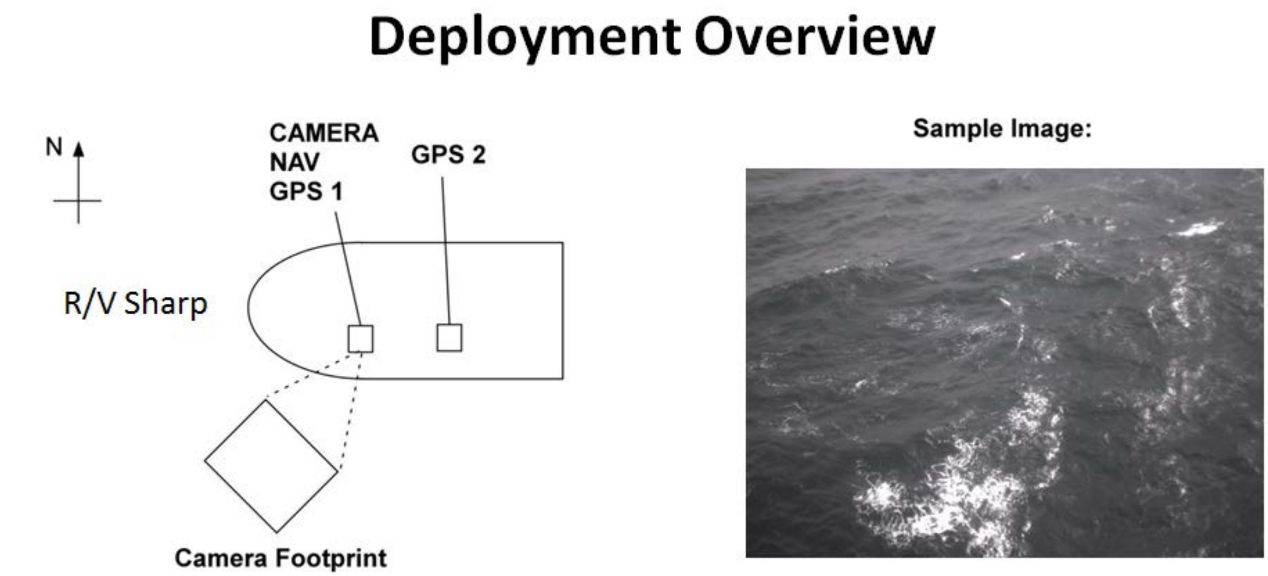

Figure 1. A schematic showing an overview of the camera deployment and a sample image showing a single whitecap. Diagram on the left shows the positions of GPS units and the primary imaging camera on the R/V Sharp. The image on the left shows a whitecap created by a breaking wave.

Whitecap images like the one shown on the right hand side of Fig. 1 were analyzed into time series of whitecap coverage prior to this project. Figure 2 shows a 10-minute time series of whitecap coverage determined from an analysis of the video data. The video frame rate was sufficiently high (~6 frames per second) that the formation and decay of breaking events can be distinguished. The peaks evident in the time series are changes in surface albedo from individual whitecaps. The expanded time series view in the bottom plot of Fig. 2 shows that the temporal resolution of individual breakers is sufficient to distinguish whitecap injection and decay times.

Analysis Methodology

The images were analyzed using 3 key algorithms. The first algorithm is an image processing technique described by Callaghan and White[2] to dynamically threshold images and determine the fraction of the image covered by a whitecap. This algorithm generated the time series shown in Fig. 2. The second algorithm was a breaking wave event detector, based on a hysteresis analysis of the whitecap fraction time series, which divided the whitecap time series into discrete breaking events. This phase of the analysis was initially performed across an entire image, but it was found that the image footprint was sufficient large that the simultaneous, small-scale breaking events occurred frequently. This problem was overcome by dividing the image into 4 sub-images and tracking whitecaps within each of them, which required redoing the whitecap analysis for each sub-image. A tracking algorithm was devised to detect the overlap of a single breaking event between two sub-images and avoid double counting.

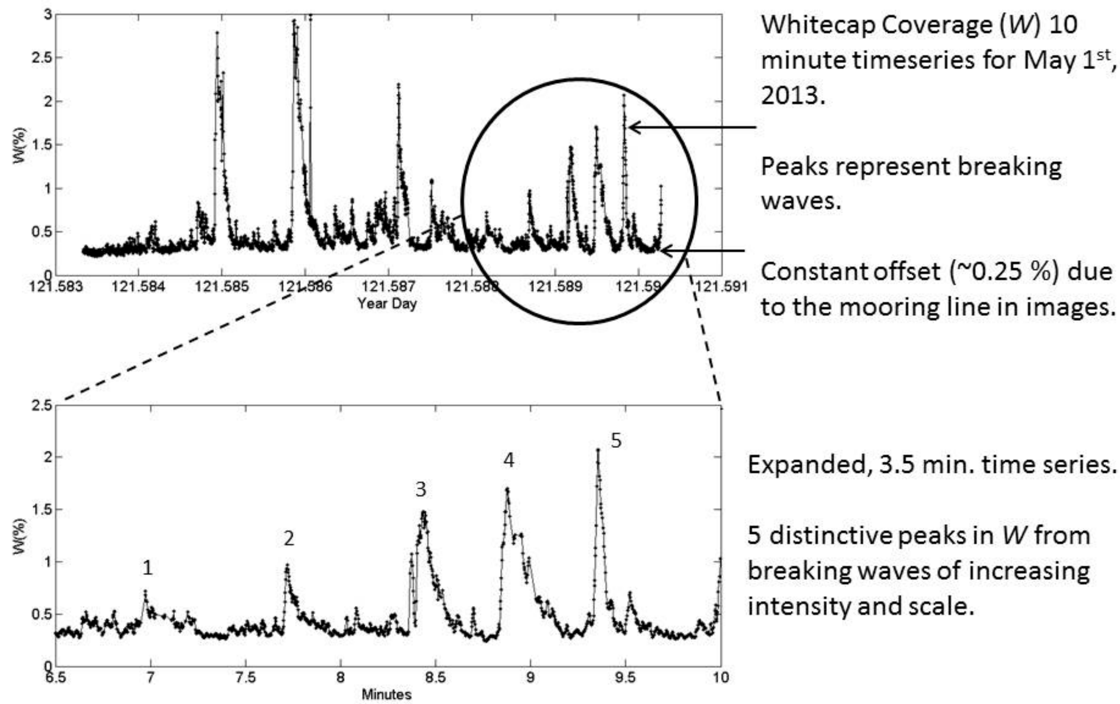

Figure 2. Time series of whitecap fraction on two different time scales from the TREX13 campaign. Whitecaps show up as increases in W that persists for a few 10's of seconds. The top plot shows 10 minutes of data and the occurrence of roughly 15 breaking events of different scale. The bottom plot shows an expanded segment of data, illustrating the growth and decay phases of whitecap foam. Values of W are offset by an approximately constant value of 0.25% because of a mooring line that appeared in the images.

Once detected, individual events were fit to a generalized functional form using a least mean square error algorithm to determine whitecap rise time, decay time and event scale. The general function used was:

$$A = \begin{cases} 0, & t < t_0 \\ A_0 \dfrac{(t - t_0)}{t_r}, & t_0 \le t < t_0 + t_r \\ A_0 e^{\frac{-(t - t_0 - t_r)}{t_f}}, & t_0 + t_r < t \end{cases} \tag{1}$$

where A_0 is the maximum event area, t is time, t_0 is the time of the onset of breaking, and t_r, t_f are the event rise and fall times. This function allows for a linear increase in whitecap area after initial wave overturning, followed by an exponential decay phase. There are 4 parameters to be fitted and this was done with a canned multivariable optimization routine available in Matlab. An example of a function fit is shown in Fig. 3.

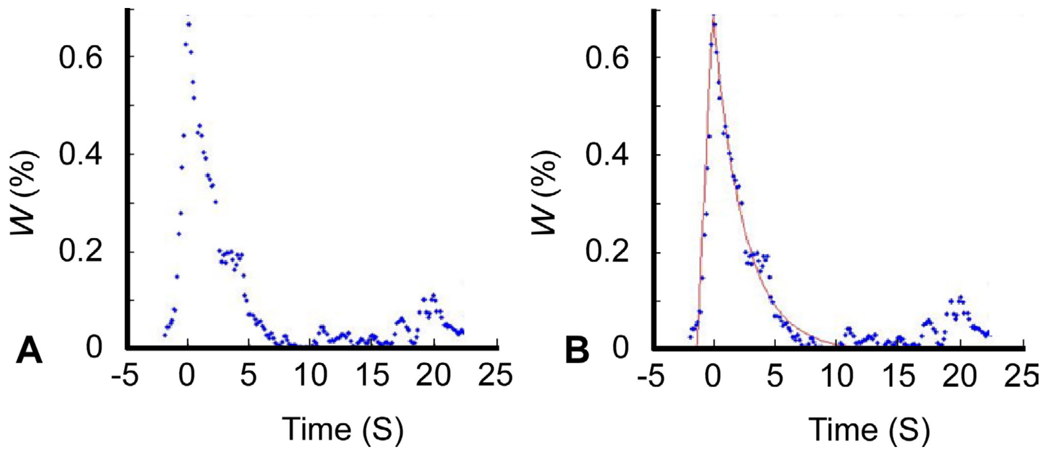

Figure 3. A. An extracted whitecap event. B. The least mean squares fit to the event (red line) superposed on the data.

WORK COMPLETED

The whitecap analysis as described above has been applied to the entire TREX13 whitecap dataset, and a total of approximately 9,800 breaking events analyzed for sampling periods ranging from 2 – 8 hours over 10 days. Wind speed during the periods of data collection ranged from 4 – 14 ms^{-1}. A summary of the whitecap analysis is shown in Fig. 4.

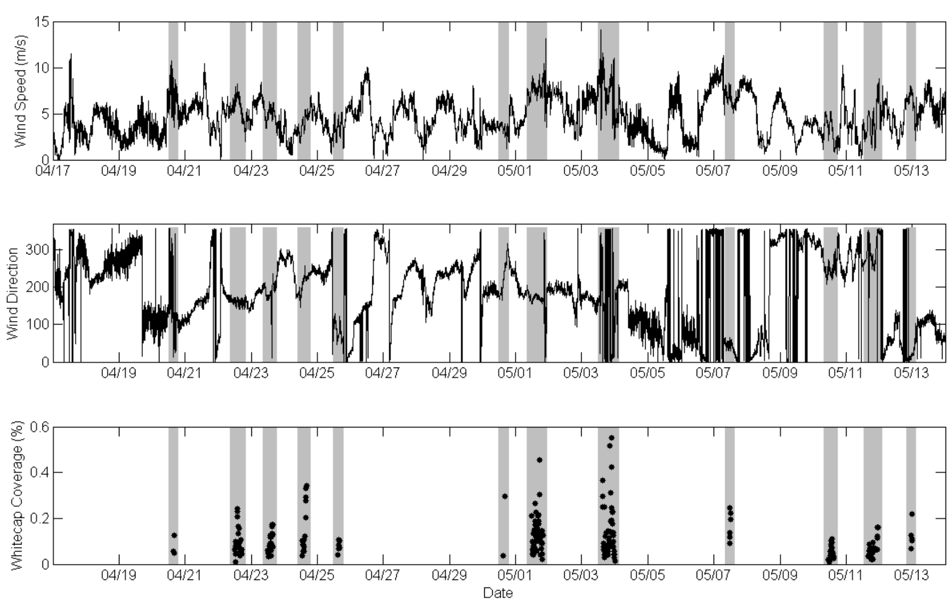

Figure 4. A summary plot of wind speed, wind direction and whitecap coverage from the TREX13 breaking wave dataset.Vertical, gray bands show where surface image data is available and has been processed. The R/V Sharp was in port on March 5th, so the data from that day was collected in very shallow water.

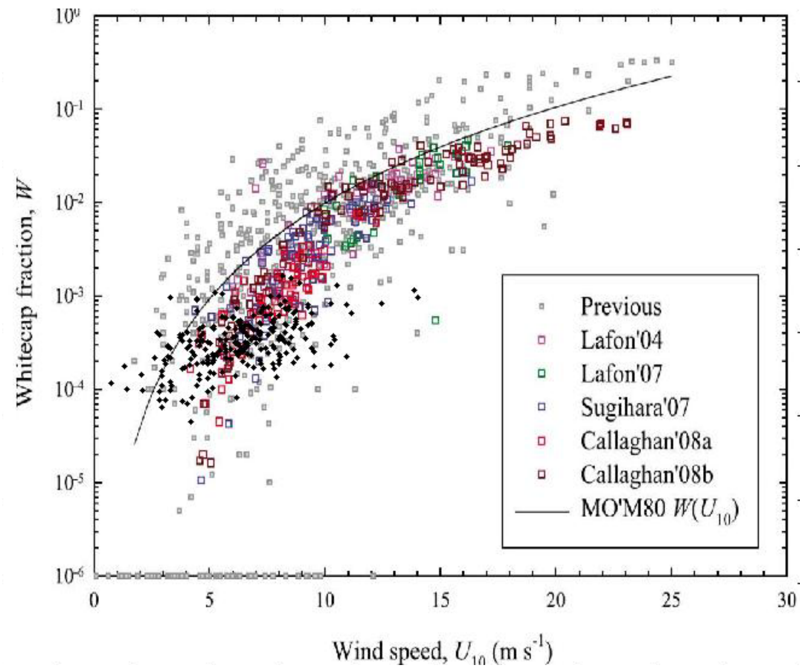

Figure 5. Whitecap data analyzed for the TREX13 expeirment plotted as a function of wind sped (black dots). Historical data from a number of other studies are also shown. The trend in whitecapping at the TREX13 site is comparable to earlier studies from open ocean sites for wind speeds in the range 2 – 6 m s^{-1}. At higher wind speeds, whitecapping is reduced relative to hisorical datasets. The very highest values occurred on March 5th, while the Sharp was in port.

Wave breaking rate as a function of wind speed is shown in Fig. 6. This parameter is particularly important, as it describes the rate at which the sea surface is overturned by wave breaking and thus the mean interval between bubble injection events. This key parameter can be used to drive a model for bubble injection and degassing in the upper ocean boundary layer[1].

The final summary of work completed consists of probability density distributions of whitecap amplitude, rise time and fall time (Fig. 7). These fitted parameters, when combined with wave breaking rate, can be used to model bubble persistence near the sea surface. Bubble persistence is expected to be a sensitive function of bubble size and wind speed, for wind speeds below ~13 m s^{-1}[1]. A further analysis of the data (not presented here) shows that whitecap injection time and decay time are relatively insensitive to wind speed, although whitecap scale is not.

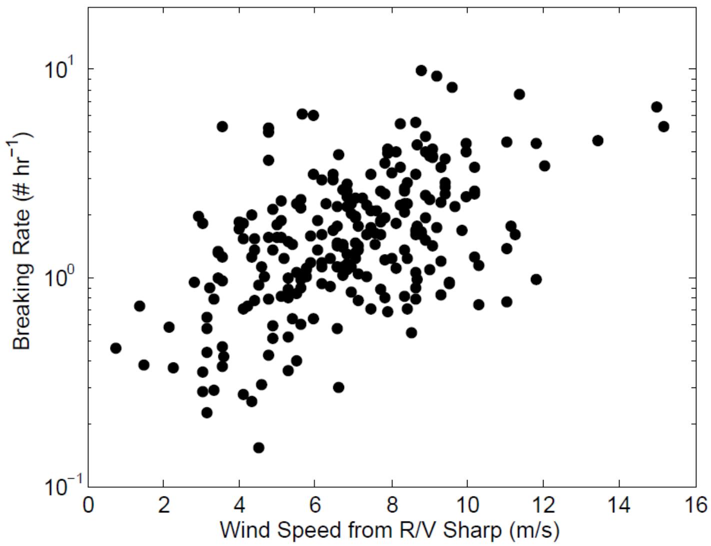

Figure 6. Wave breaking rate in events per hour as a function of wind speed. Breaking rates vary from less than 1 per hour to more than 10 per hour across the wind speed range 2 – 10 m s^{-1}. As with whitecap coverage, these rates tend to be somewhat lower than those reported in the literature for comparable wind speeds[3].

Work yet to be completed is the incorporation of the whitecap parameterizations into an analysis of surface scattering. Conversations with Principal Investigators who collected surface reverberation data during the experiment are underway, and this work will be complete by the end of the project.

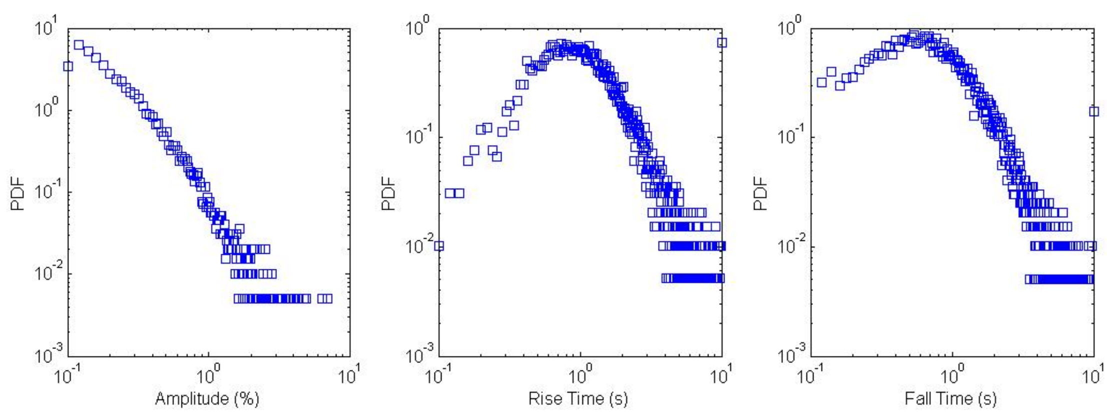

Figure 7. Probability density distributions of whitecap amplitude, rise time and fall time from the TREX13 experiment. The data summary includes all events across all wind speeds. The amplitude distribution is dominated by small-scale events. Rise and fall time distributions show a broad peak at around 1 s and 0.7 s respectively.

RESULTS

There are two main results to report at this stage of the project. The first is the development of an image processing algorithm capable of estimating whitecap scale, injection time and decay time from video imagery of the sea surface. This is the first time such an automated algorithm has been attempted and successfully executed in either the acoustics or oceanographical communities. The application of this software to other whitecap datasets (such as the KAM11 campaign of Hawaii in 2011) could provide valuable information about wave breaking activity and sub-surface bubble activity, which are important for understanding the interaction of sound with the wind-driven sea surface, the optical properties of the near surface boundary layer, and the production of marine aerosols which form condensation nuclei.

The second main result is the extraction of breaking wave parameters during the TREX13 experiment, which will be used to help interpret surface reverberation measurements from that campaign. The processing of 9,800 whitecaps is summerized in Figs. 4 through 7.

The result that whitecap coverage and wave breaking rates for TREX13 are lower than those typically observed in the open ocean underlines the importance of taking surface observations of whitecaps when trying to quantify the effects of bubbles on surface scattering. Using the whitecap parameterization shown in Fig. 5 would result in a gross overestimate of wave breaking and air entrainment during this experiment.

IMPACT/APPLICATIONS

Bubbles entraind by breaking waves are an integral component of the wind-driven sea surface, with implications for surface reverberation, remote sensing of the sea surface, ocean color and marine aerosols. State of the art models for bubble entrainment date back to the 1990's and it is time they were updated. New models must be driven by a combination of observation and theory, and the work of this project is a first step in that direction. The direct application of this work will be tested with collaborating PI's who measured surface reverberation during TREX13.

RELATED PROJECTS

None.

REFERENCES

[1] Deane G.B., J.C. Preisig and A.C. Lavery, 2013. "The suspension of large bubbles near the sea surface by turbulence and their role in absorbing forward-scattered sound," IEEE J. Ocean. Eng. 38(4) 632-641.

[2] Callaghan, A. H., and M. White, 2009. "Automated processing of sea surface images for the determination of whitecap coverage." *Journal of Atmospheric and Oceanic Technology* 26(2) 383-394.

[3] Gemmrich, J. R., M. L. Banner, and C. Garrett, 2008. "Spectrally resolved energy dissipation rate and momentum flux of breaking waves." *Journal of Physical Oceanography* 38(6) 1296-1312.